

Manipulation of Crystal Shape by Cycles of Growth and Dissolution

Ryan C. Snyder, Stephan Studener, and Michael F. Doherty

Dept. of Chemical Engineering, University of California, Santa Barbara, CA 93106

DOI 10.1002/aic.11174

Published online April 30, 2007 in Wiley InterScience (www.interscience.wiley.com).

A method for the manipulation of crystal shape by using cycles of growth and dissolution is presented, representing a unique process-based solution to an important product quality concern. Using 3-D shape evolution models for faceted crystal growth and dissolution, results are reported for cycling both an illustrative crystal system, as well as a physical plate-like system. The results show that crystal shape can be manipulated by cycling when the relative growth and dissolution rates are anisotropic, which can be caused by differences in growth mechanism, asymmetry in super/undersaturation, and by the use of surface active additives. Since this method of crystal shape enhancement uses the existing liquid solution, it could be a valuable alternative to the traditional methods which often require changes in the chemical nature of the solution, for example, by changing solvent. © 2007 American Institute of Chemical Engineers AIChE J, 53: 1510–1517, 2007

Keywords: crystal growth, dissolution, morphology, shape evolution

Introduction

In recent years, a major focus of chemical engineering has been the emphasis on product design and its integration into traditional process design methodologies.¹ This focus on products is largely driven by the growing importance of microstructured materials which possess unique properties and performance specific to the internal lattice structure, and are commonly found in the food, pharmaceutical and electronics industries. For crystalline products, these properties are often specific to each crystal face; therefore, the size of each crystal face and, hence, the crystal shape is of critical importance. For example, given a crystal with a single face of particularly high-catalytic activity, the area of such a face should be maximized; however, for a crystal, such as adipic acid where the hydrophobicity of the (100) face makes bulk transport difficult, the area of that face should be minimized. Additionally, crystal shape affects both downstream processes, such as filtering, washing and drying, as well as mechanical strength.

Most industrial crystallizations take place in solution; therefore, existing efforts in engineering enhanced crystal shapes primarily rely directly upon changing the chemical nature of the crystallization. Different solvents lead to different crystal shapes, and mixed solvents can lead to even more flexibility. For example, the aspect ratio of ibuprofen has been shown to be directly correlated to the polarity of the solvent.² Additives, both tailor made and surfactants, have also been used to chemically alter the shapes that crystals can achieve.^{3,4} In each of these cases, the change of the chemical nature of the solution requires the use of additional chemicals, and may also require additional recrystallizations or separations, leading to possible complications in process design and operation. Here, we present a novel processing scheme that could lead to enhanced crystal shapes, hence, solving a product quality problem solely by process engineering. Such a nonchemical route to crystal shape enhancement has the benefit of not requiring changes in solvent, or additional impurities or separations since it uses the existing liquid mixture already available in the process.

We propose to manipulate the shape of faceted crystals by using repeated cycles of growth and dissolution. Using existing models for both faceted growth⁵ and dissolution,⁶ we show that conducting cycles of dissolution and growth can

Correspondence concerning this article should be addressed to M. F. Doherty at mfd@engineering.ucsb.edu.

be a valuable mechanism for generating crystal shapes that are not obtainable through either growth or dissolution alone. This article is organized as follows. We begin by describing the background to the growth and dissolution shape evolution models. Then, we describe a discrete dynamical model that tracks the change in crystal shape at the end of each cycle of dissolution and growth. Next, we derive the conditions for which a change in crystal shape occurs via cycles of growth and dissolution. Finally, we use both an illustrative crystal system, as well as the physical plate-like system similar to succinic or adipic acid to demonstrate the impact of implementing cycles of growth and dissolution on the shape of a single crystal.

Modeling Growth and Dissolution

A method for modeling the faceted shape evolution of either a growing⁵ or a dissolving⁶ crystal has been developed. This model tracks the relative perpendicular distance from an origin inside the crystal to each face by a system of ordinary-differential equations. The differential equations are coupled to a set of algebraic conditions that determine when faces appear at edges or vertices as the shape of the crystal evolves in time. In addition, a set of rules governs the total superset of planes that are to be considered during the evolution. The model inputs are the crystallography, as well as the relative growth and dissolution rates of each face, which can be taken from either experimental data or models. It is important to note that only the relative growth and dissolution rates are needed to model crystal shapes. In our formulation, all of the growth rates are normalized to the slowest growing face, and all of the dissolution rates are normalized to the slowest dissolving face; therefore, all of the relative rates are greater than or equal to unity.

Let H_i denote the perpendicular distance of face i from a center point in the crystal, and let G_i denote its normal velocity, then H_i and G_i are related by

$$\frac{dH_i}{dt} = G_i, \quad i = 1, \dots, N \quad (1)$$

This differential equation describes the growth of face i when $G_i > 0$, and the dissolution of face i when $G_i < 0$. In the following, “Growth” will be denoted by the subscript “G”, while “Dissolution” will be denoted by the subscript “D”. Let the perpendicular distance of a reference face H_{ref} , be the characteristic length of the crystal, $G_{G,\text{ref}} = \frac{dH_{\text{ref}}}{dt}$ be the characteristic-growth velocity, and $G_{D,\text{ref}} = \frac{dH_{\text{ref}}}{dt}$ be the characteristic-dissolution velocity. Then, the dimensionless perpendicular distance is $x_i = H_i/H_{\text{ref}}$, the relative (dimensionless) growth velocity is $R_{G,i} = G_{G,i}/G_{G,\text{ref}}$ and the relative (dimensionless) dissolution velocity is $R_{D,i} = G_{D,i}/G_{D,\text{ref}}$. By introducing a “warped” time for growth, $d\xi_G = \frac{G_{G,\text{ref}}}{H_{\text{ref}}} dt$ Eq. 1 can be recast in fully dimensionless form for growth:

$$\frac{dx_i}{d\xi_G} = R_{G,i} - x_i, \quad i = 1, \dots, N-1 \quad (2)$$

If the relative growth rates are constant, the model is a linear system of ordinary-differential equations, and all of the

eigenvalues are equal to -1 ; therefore, the unique and stable steady-state is

$$x_i = R_{G,i}, \quad i = 1, \dots, N-1 \quad (3)$$

which the system will evolve towards during growth. Similarly, for dissolution, a “warped” time is defined as $d\xi_D = -\frac{G_{D,\text{ref}}}{H_{\text{ref}}} dt$ where the negative sign is introduced since the reference dissolution rate is negative, and the “warped” time should increase as time increases. Again, Eq. 1 can be recast in dimensionless form, in this case for dissolution:

$$\frac{dx_i}{d\xi_D} = x_i - R_{D,i}, \quad i = 1, \dots, N-1 \quad (4)$$

Assuming all the relative rates of dissolution are constant, Eq. 4 is a linear system of ordinary-differential equations with eigenvalues all equal to $+1$. Thus, the steady-state, $x_i = R_{D,i}$, is unstable, and the system will move away from the steady-state during dissolution. For both growth and dissolution, these sets of differential equations are coupled to a set of rules for selecting candidate faces, as well as to an algebraic condition that determines when new faces may appear. A full description of these rules is presented in Zhang et al.⁵ and Snyder and Doherty.⁶

In general, the relative rates of growth and dissolution, $R_{G,i}$ and $R_{D,i}$, will depend on the actual conditions inside the crystallizer (for example, supersaturation, undersaturation or concentration of impurities) and may not be constant. Thus, Eq. 2 or Eq. 4 should be coupled to the crystallizer mass and energy balances, causing the system to be nonlinear.

Discrete Dynamic System

The differential equations describing growth and dissolution track the relative perpendicular distance continuously in time; however, we are primarily interested in the result of a change in shape after a complete cycle of dissolution and growth. Thus, a discrete dynamical system describing the resulting shape change after the end of each cycle is desired. For the case of constant relative growth and dissolution rates, the solutions of the growth equations are

$$x_i(\xi_G) = R_{G,i} - (R_{G,i} - x_i(0)) \cdot \exp\{-\xi_G\}, \quad i = 1, \dots, N-1 \quad (5)$$

$$\xi_G = \ln\left(\frac{H_{\text{ref}}(t_G)}{H_{\text{ref}}(0)}\right) \quad (6)$$

and the solutions to the dissolution equations are

$$x_i(\xi_D) = (x_i(0) - R_{D,i}) \cdot \exp\{\xi_D\} + R_{D,i}, \quad i = 1, \dots, N-1 \quad (7)$$

$$\xi_D = \ln\left(\frac{H_{\text{ref}}(0)}{H_{\text{ref}}(t_D)}\right) \quad (8)$$

The relative perpendicular distance to face i at the end of cycle j is defined as $x_{i,j}$, thus, the initial condition to any cycling scheme is given by $x_{i,0}$. First, begin with a crystal face with perpendicular distance $x_{i,j}$, and dissolve it for a time

Δt_D corresponding to a dimensionless time $\Delta \xi_D$. Substituting these conditions into Eq. 7 the perpendicular distance of each face i after warped time $\Delta \xi_D$ is given by

$$x_i(\Delta \xi_D) = (x_{i,j} - R_{D,i}) \cdot \exp\{\Delta \xi_D\} + R_{D,i}, \quad i = 1, \dots, N-1 \quad (9)$$

Then, grow the crystal for a time Δt_G corresponding to a dimensionless time $\Delta \xi_G$. Substituting $x_i(\Delta \xi_D)$ from Eq. 9 as the initial condition of Eq. 5 results in an expression for $x_{i,j+1}$

$$x_{i,j+1} = R_{G,i} - (R_{G,i} - R_{D,i} - (x_{i,j} - R_{D,i}) \cdot \exp\{\Delta \xi_D\}) \cdot \exp\{-\Delta \xi_G\} \quad (10)$$

This defines the recursive relationship between the relative perpendicular distance from one cycle $x_{i,j}$ to the next $x_{i,j+1}$, and, hence, defines the discrete dynamical system describing the shape after each cycle. This is only valid for the case when relative growth and dissolution rates are constant, and when none of the growth faces disappear from the crystal during the dissolution stage. (Since faces that have disappeared no longer have a real growth or dissolution rate, they are not constant.)

Now consider the case where the relative rates of growth and dissolution are all equal such that

$$R_{G,i} = R_{D,i} = R_i, \quad i = 1, \dots, N-1 \quad (11)$$

Equation 10 then simplifies to

$$x_{i,j+1} = R_i + (x_{i,j} - R_i) \cdot \exp\{\Delta \xi_D - \Delta \xi_G\}, \quad i = 1, \dots, N-1 \quad (12)$$

When the dimensionless “warped” times, $\Delta \xi_D$ and $\Delta \xi_G$ are equal (that is, the fractional decrease in crystal size by dissolution equals the fractional increase in size due to growth), Eq. 12 simplifies to

$$x_{i,j+1} = x_{i,j}, \quad i = 1, \dots, N-1 \quad (13)$$

and there is no change in the relative perpendicular distance after a complete cycle. Therefore, growth and dissolution are reversible, and there is no change in crystal shape or size as a result of the cycling process. Thus, in order for a shape change to be achieved during cycling either the relative rate of growth and dissolution must be unequal for at least one face, or $\Delta \xi_D \neq \Delta \xi_G$. This difference can occur in one of several ways. First, the relative rates of growth and dissolution could simply be unequal for at least one face i . Alternatively, as mentioned earlier, one of the faces that was present at the beginning of the cycle could disappear during the dissolution stage of the process. Thus, this “real” face will have degenerated into a “virtual” face, and will no longer travel at the same relative rate. Finally, one or more of the relative growth and dissolution rates may not be constant, which would immediately make the equations nonlinear and irreversible.

Quantifying Changes in Crystal Morphology

Monitoring changes in crystal shape requires tracking the area or perpendicular distance of each crystal face. Alternatively

a single quantity, such as the sphericity, can be used to conveniently determine changes in crystal shape after cycling. The sphericity ψ is defined as the ratio of the surface area of a sphere with a volume identical to that of the crystal, to the actual surface area of the crystal. This can be expressed as

$$\psi = \frac{\sqrt[3]{36 \cdot \pi \cdot V_{\text{crystal}}}}{S_{\text{crystal}}} \quad (14)$$

where V_{crystal} is the crystal volume, and S_{crystal} is the crystal surface area. Thus, for isometric particles ψ is close to one (for a sphere it is equal to one) while for crystals that are needle-like or plate-like its value is much lower.

Results: Illustrative System

First, we report results of cycling an illustrative crystal system which demonstrate the possible morphological changes resulting from cycles of dissolution and growth. The illustrative crystal system contains a single growth unit per unit cell with the unit cell parameters $a = b = c = 1$ and $\alpha = \beta = \gamma = 90^\circ$. There are three sets of flat planes in the illustrative system corresponding to the {100}, {010} and {001} plane families. The relative growth and dissolution rates of the {010} plane family are different from those of the {100} and {001} plane families. The relative growth rates of the {010} families of planes are set at three, while the relative growth rates of the {100} and {001} families of planes are set at one. There are twelve planes at the edges of the adjacent flat planes corresponding to the {011}, {101} and {110} plane families, and there are eight planes at the vertices corresponding to the {111} plane family. Since these are stepped or kinked planes, their relative growth and dissolution rates are set to 10 (an order of magnitude higher than the slowest growing faces). These planes are potential dissolution planes or faces, and are not present on either the steady-state growth habit or the steady-state dissolution habit. These planes also comprise the entire superset necessary to describe growth and dissolution of this illustrative system.⁶ When these relative growth and dissolution rates are put into the dynamic model they describe the shape evolution during each cycle. During a growth stage, shapes will evolve toward the steady-state growth shape which is displayed in Figure 1a. This shape is used as the initial condition for beginning the cycling protocol for each simulation.

First, consider the case where the relative rates of growth and dissolution are equal. The operating policy for this simulation is to first dissolve 20% of the crystal volume, then to grow until the original volume has been reattained. Figure 1b shows the crystal shape when 20% of the crystal is dissolved, and none of the growth faces have yet disappeared from the surface of the crystal. Figure 2 shows the continuous course of the sphericity for this process. The crystal shapes at the beginning and end of each stage of dissolution and growth are shown on the figure. During dissolution, the crystal becomes more faceted, its surface area increases, thus the sphericity initially increases. Once the crystal begins to grow, a discontinuity in slope is seen. Then, the evolution of the crystal follows the same relative trajectory in reverse as during dissolution. When the crystal is regrown to its initial

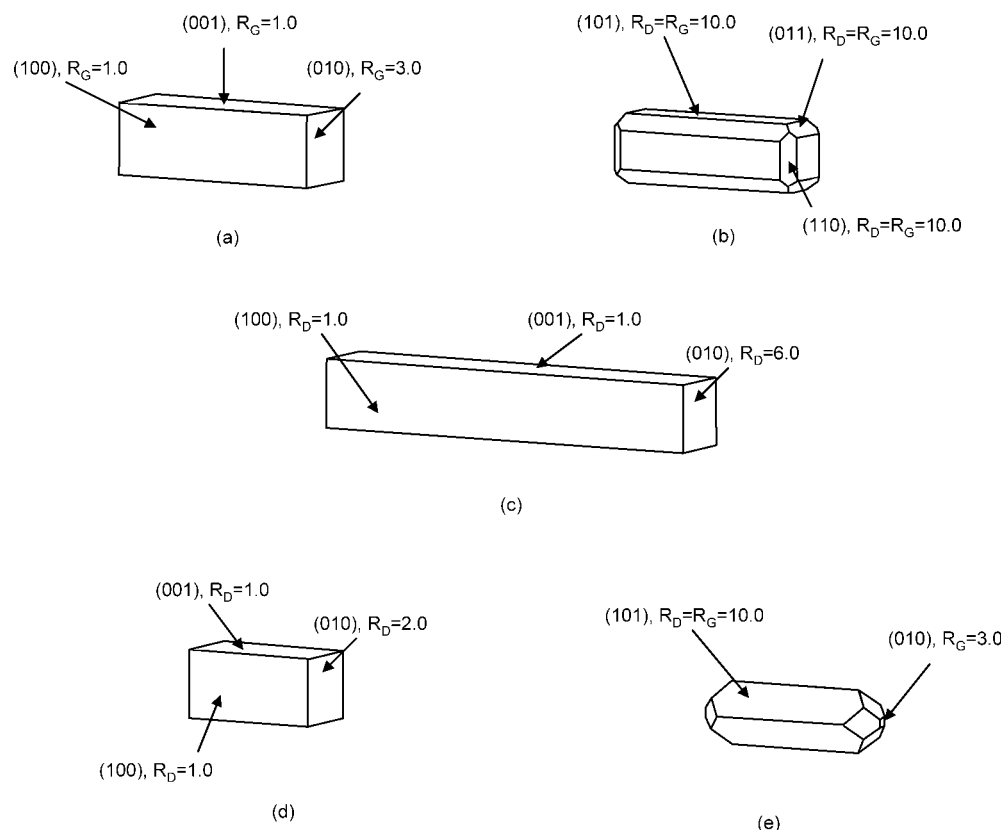


Figure 1. Illustrative system crystal habits: growth steady-state (a); 20% of the initial volume dissolved when $R_{G,i} = R_{D,i}$, note that none of the growth faces disappear (b); the unstable dissolution steady-state for $R_{D,\{010\}} = R_{D,\{0\bar{1}0\}} = 6.0$ (c); the unstable dissolution steady-state for $R_{D,\{010\}} = R_{D,\{0\bar{1}0\}} = 2.0$ (d); 65% of the initial volume dissolved when $R_{G,i} = R_{D,i}$, note that some of the growth faces have disappeared (e).

volume, a cycle is completed and its sphericity is again equal to ψ_{ss} . The actual time required to follow the trajectory is not enumerated here, since only relative rates of growth and dissolution, and dimensionless time are required in the simulation. (Recall that the dimensionless time is a measure of the change of crystal volume.) The dimensionless time at the end of each cycle is noted by the integers 1, 2, ..., and the end of each dissolution stage is marked by 1d, 2d, ... in the figures. The real duration time, in minutes, of each stage of the cycle depends on the absolute dissolution and growth rates; therefore, these duration times can be different even in the case when the dimensionless duration times are equal. Since absolute dissolution rates are normally higher than absolute growth rates, the real-time required to dissolve 20% of the crystal's volume will often be shorter than the real-time required to grow 20% of the crystal's volume.

As predicted from the discrete dynamical system, the process is reversible when the relative rates of growth and of dissolution are equal for every face and none of the growth faces disappear from the surface of the crystal. To break the reversibility, first the relative rates are chosen to be different. Later, we consider the case of breaking reversibility as a result of the disappearance of some of the growth faces. The relative rates of growth and the relative rates of dissolution could be different for a number of reasons, for example, different mechanism of growth and dissolution (2-D-nucleation vs spi-

ral growth), different super/undersaturation effects or impurities affecting growth but not dissolution of faces. However, it depends strictly on whether the relative rate of dissolution of a face i is larger or smaller than its relative rate of growth as to which shapes are attainable by cycling.

First, the relative rates of dissolution of the $\{010\}$ family of planes are chosen to be larger than the relative rates of growth ($R_{D,\{010\}} = R_{D,\{0\bar{1}0\}} = 6$). The other faces each have the same relative growth and dissolution rates ($R_{D,\{100\}} = R_{G,\{100\}}$, $R_{D,\{001\}} = R_{G,\{001\}}$, $R_{D,\{011\}} = R_{G,\{011\}}$, $R_{D,\{101\}} = R_{G,\{101\}}$, $R_{D,\{110\}} = R_{G,\{110\}}$ and $R_{D,\{111\}} = R_{G,\{111\}}$). These rates now describe the new dynamics during the dissolution stage of the cycling protocol. The shape of the unstable dissolution steady-state (Figure 1c) is different from the stable growth steady-state. During the cycling process, while shapes are dynamically dissolving they will evolve away from the steady-state dissolution shape, and while shapes are growing they will dynamically evolve towards the steady-state growth shape.

The policy for this cycling process is to dissolve 20% of the crystal's material and regrow it to the original volume. For this degree of dissolution, growth faces do not disappear during dissolution. Figure 3 shows the continuous course of the sphericity as the crystal is cycled through multiple stages of dissolution and growth. Within each period of growth, a new discontinuity in slope exists (as seen at the end of each growth period) corresponding to the disappearance of some

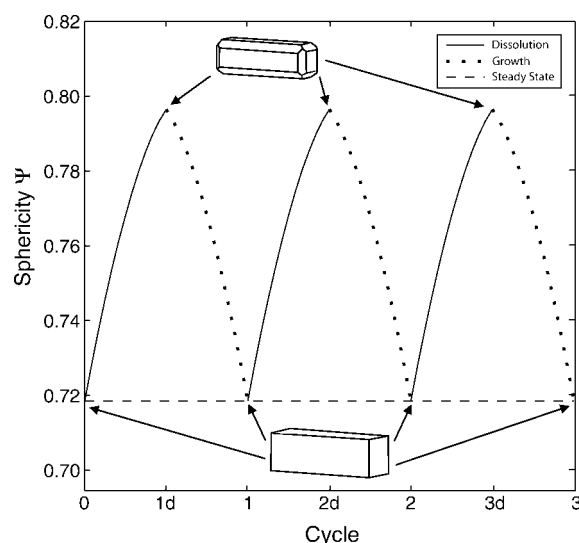


Figure 2. The sphericity evolution of the illustrative system for the case when $R_{G,i} = R_{D,i}$ for each face, i .

Note that since none of the growth faces disappear through the end of each dissolution stage, growth and dissolution are reversible. Thus, the sphericity and habit both return to their steady-state value after each cycle.

of the dissolution planes from the habit. Since the relative rates of growth and dissolution are no longer equal, the sphericity does not return to its steady-state value at the end of a cycle; hence, the shape has changed as a result of the cycling procedure. Note that the location of the points 1d, 2d, ... are no longer midway within the cycles. Figure 4 shows the discrete sphericity evolution at the end of each cycle of dissolution and growth. Several crystal habits are also included to visualize the result of the shape change. As cycling proceeds,

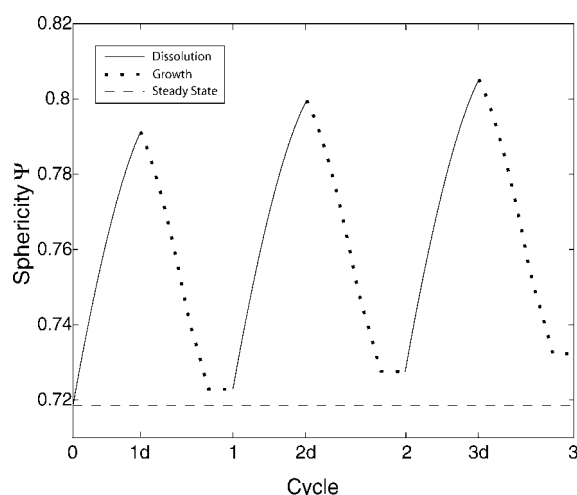


Figure 3. The sphericity evolution of the illustrative system for the case when $R_{D,\{010\}} = R_{D,\{0\bar{1}0\}} = 6.0$.

For each of the other faces $R_{G,i} = R_{D,i}$.

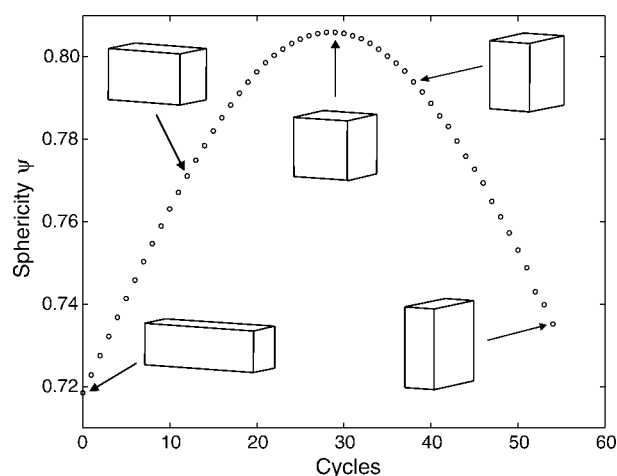


Figure 4. The sphericity of the illustrative system after each cycle for the case when $R_{G,\{010\}} > R_{D,\{010\}}$.

The crystal habit is flattened as cycling proceeds and the sphericity obtains a maximum when the system achieves a cubic shape.

the perpendicular distance becomes smaller for the $\{010\}$ planes. This can be understood by comparing the shapes to the steady-states of both growth and dissolution. During the dissolution stage the crystal moves away from its steady-state dissolution shape; thus, it is dramatically shortened in the $[010]$ and $[0\bar{1}0]$ direction since the relative dissolution rates of those faces are increased. When it is regrown it evolves toward the steady-state growth shape, and is elongated only partially to the extent that it was shortened in the dissolution stage. Thus, the resulting shape has the net change of being less like the steady-state dissolution shape. As the process of cycling continues, the sphericity reaches a maximum when the habit is a cube, and then decreases as the habit becomes more plate-like.

Now consider the case when the relative rates of dissolution of the $\{010\}$ family of planes are chosen to be smaller than their relative rates of growth ($R_{D,\{010\}} = R_{D,\{0\bar{1}0\}} = 2$), while the other faces again have equal relative growth and dissolution rates. The unstable dissolution steady-state for this case is shown in Figure 1d. In this case, the habit of the dissolution steady-state is less elongated than the steady-state for growth. Thus, since the crystals become less like their steady-state dissolution shape during cycling, it is expected that the crystals in this case will become more needle-like as a result. Again the system is initialized with the steady-state growth shape. Figure 5 shows the sphericity evolution at the end of each cycle along with selected crystal habits at specific cycle points. In this case, 20% of the crystal volume was dissolved in each dissolution stage, and the crystal was regrown until only growth faces were present on the crystal habit. (If the crystal is only regrown to its original volume, some dissolution faces are still present on the habit making shape comparison more challenging.) As expected, the crystal becomes more extended in the $[010]$ and $[0\bar{1}0]$ direction, resulting in a more needle-like crystal with a continually decreasing sphericity.

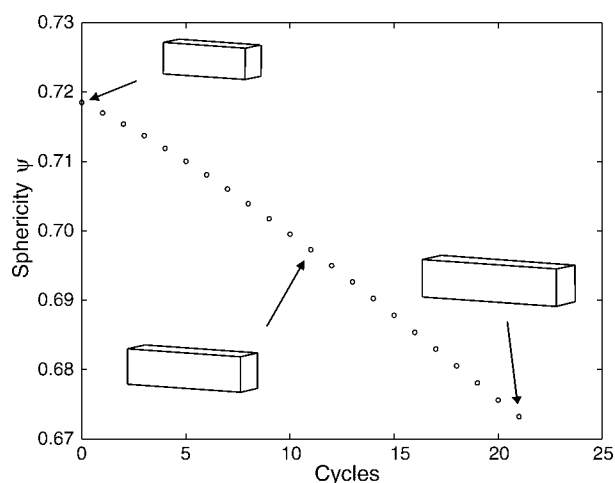


Figure 5. The sphericity of the illustrative system after each cycle for the case when $R_{G,(010)} < R_{D,(010)}$.

The habit is elongated as cycling proceeds.

When relative rates of growth and dissolution are equal, the cycling process also becomes irreversible when the crystal is dissolved to the point where some of the growth faces have disappeared. When they disappear they degenerate as a vertex or edge, thus, they have no real velocity and they move with a virtual velocity corresponding to that of the vertex or edge. Thus, their relative rate of dissolution becomes different from their relative rate of growth for a portion of the cycling process, leading to a change in shape. In the illustrative system, faces disappear when approximately 65%

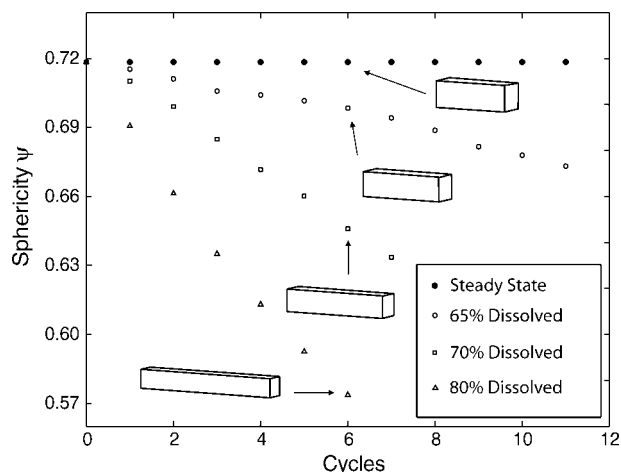


Figure 6. Sphericity of the illustrative system is shown after each cycle for various amounts of crystal dissolution during each dissolution stage.

The crystal cycling reversibility is broken solely as a result of some of the steady-state growth faces disappearing during each dissolution cycle. The habit at the end of the sixth cycle in each case is also shown.

of the material has been dissolved. The corresponding habit is displayed in Figure 1e. When 80% of the crystal has been dissolved, all the growth faces have vanished from the surface of the crystal. The magnitude of change in crystal shape depends on the amount of material dissolved during a period of dissolution, since this determines which faces disappear during dissolution and when they reappear during growth. Several simulations are now reported, each is initialized with the steady-state growth shape, then a specific percentage of the material is dissolved, and the crystal is regrown to its original volume. Figure 6 shows the sphericity at the end of each cycle for multiple values of the amount of material dissolved during each dissolution stage. Note that as the amount of material dissolved in each dissolution stage increases, the magnitude of the shape change also increases. In each case, the system becomes elongated in the $[010]$ and $[0\bar{1}0]$ direction.

Results: Plate-like systems

The results in the previous section highlight the conditions under which a shape change occurs during a cycle of growth and dissolution. Now we present the results for a cycling simulation of a physical crystal system, with a hexagonal plate-like steady-state growth shape that is similar to that of both succinic and adipic acids grown in water. This hexagonal plate-like steady-state growth shape contains large $\{100\}$ faces (see Figure 7a). There are two growth units per unit cell, and the unit cell parameters are $a = 5.519\text{\AA}$, $b = 8.862\text{\AA}$, $c = 5.101\text{\AA}$, $\alpha = \gamma = 90^\circ$ and $\beta = 91.59^\circ$. There are three sets of flat planes that need to be considered for the system corresponding to the $\{100\}$, $\{011\}$ and $\{020\}$ plane families. The relative growth rates for the flat planes are set

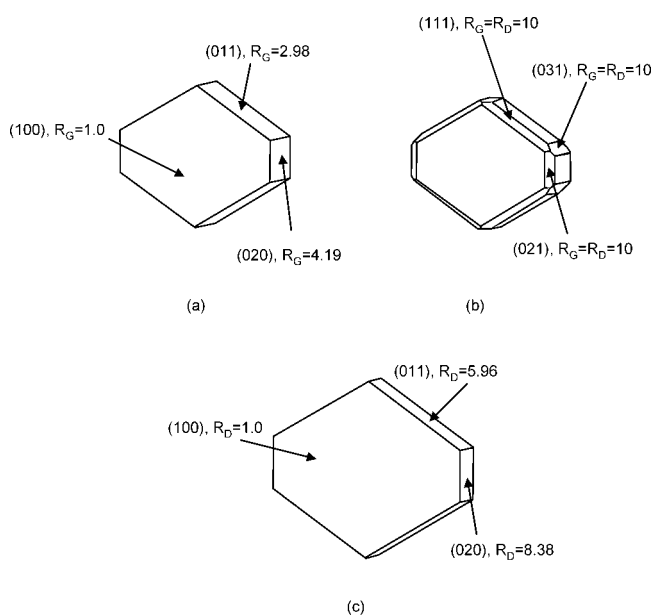


Figure 7. Plate-like system crystal habits: Growth steady-state (a), 25% partially dissolved in the initial dissolution stage (b), and the dissolution steady-state (c).

as $R_{G,\{100\}} = 1.0$, $R_{G,\{011\}} = 2.98$ and $R_{G,\{020\}} = 4.19$. The superset of planes for the growth and dissolution simulation also contains the 18 planes in the $\{1\bar{1}1\}$, $\{11\bar{1}\}$, $\{002\}$, $\{120\}$, $\{201\}$ and $\{031\}$ plane families corresponding to the planes at the edges formed by the flat faces, and the 12 planes in the $\{102\}$, $\{10\bar{2}\}$, and $\{131\}$ plane families corresponding to the planes at the vertices formed by the adjacent flat faces.⁶ These stepped and kinked faces are given relative rates of growth and dissolution an order of magnitude higher than the slowest growing face ($R_{G,i} = R_{D,i} = 10.0$).⁷

Now we demonstrate the cycling model for a set of relative dissolution rates corresponding to $R_{D,\{020\}} = 8.38$ and $R_{D,\{011\}} = 5.96$. For all of the other faces the condition $R_{G,i} = R_{D,i}$ holds. In the dissolution stage, 25% of the initial volume is dissolved which is such that none of the growth faces disappear. Thus, the resulting change in crystal morphology is purely a result of the anisotropy of the growth and dissolution rates. The crystal habit after the initial stage of dissolution with all of the growth faces still present is shown in Figure 7b. The growth stage of each cycle proceeds until the crystal attains its original volume. The unstable dissolution steady-state habit is shown in Figure 7c.

Figure 8 shows the resulting sphericity after each cycle along with selected crystal habits. During the cycling process the crystal habit becomes more block-like, which again corresponds to shapes less like the dissolution steady-state. Figure 9 shows the evolution of the relative areas of several crystal plane families. Note that the relative areas of the $\{011\}$ and $\{020\}$ plane families increase as the cycling process proceeds since both of those plane families are more important on the growth steady-state than on the dissolution steady-state. Accordingly, the relative area of the $\{100\}$ plane family decreases as time evolves, since it is less important on the growth steady-state shape than on the dissolution steady-state shape. This is in complete agreement with the idea that as the cycling evolves the crystal habit becomes less like the dissolution steady-state. If the cycling was con-

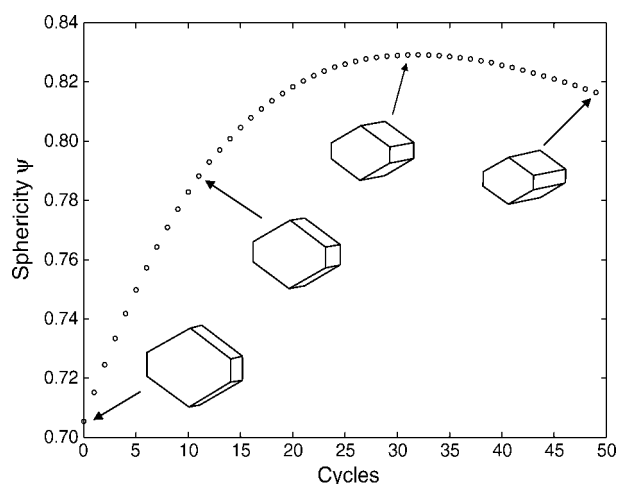


Figure 8. The sphericity of the plate-like system after each cycle is shown along with the corresponding crystal habit for several specific cycles.

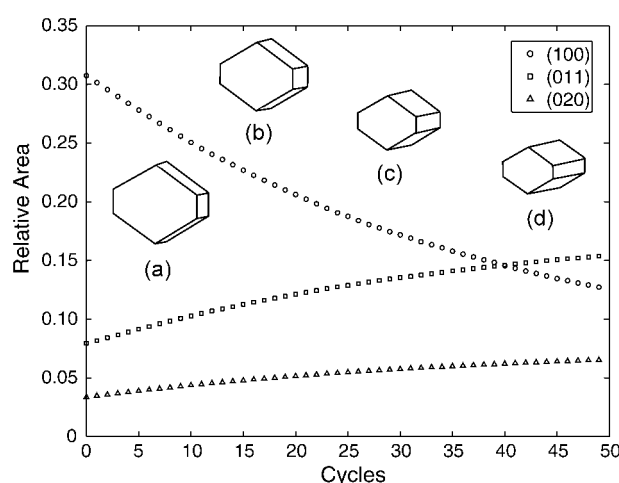


Figure 9. The relative areas of several faces of the plate-like system being cycled.

The corresponding crystal habits are shown for the steady-state (a), the 11th cycle (b), the 31st cycle (c) and the 49th cycle (d).

tinued, the habit would approach that of a needle elongated in the $\{010\}$ direction.

Conclusions

Using faceted shape evolution models, predictions of morphological enhancement due to a cycling through stages of both dissolution and growth have been reported. This enhancement of crystal shape results from the anisotropy of relative growth and dissolution rates, as well as the systematic disappearance and reappearance of crystal faces. When none of the growth faces disappear during the dissolution stage of the cycle, the result of cycling can be predicted by a comparison of the steady-states of both growth and dissolution. The shape, in general, becomes less like the dissolution steady-state as the cycling proceeds. The magnitude of the shape enhancement also depends upon the quantity of material dissolved.

While this study highlights the possibilities of such a shape enhancement protocol, in a real crystallizer a distribution of crystal sizes and shapes exists. Thus, each of the crystals are affected by the cycling to varying degrees. While larger crystals are subject to small changes in shape during a cycle, smaller crystals could even dissolve away completely. Thus, by applying cycles of growth and dissolution both the size as well as the shape of the crystal population are subject to change. Furthermore, since a large number of cycles are often necessary to produce a desired shape enhancement, the continual heating and cooling of a single batch crystallizer would be very time consuming and inefficient. (If only because of the thermal inertia of the equipment.) Rather, new crystallizer configurations are sought for accomplishing this new scheme. Such an embodiment could consist of linking two crystallizers together, with one for growth and another for dissolution, such that the slurry is circulated between them. Alternatively, a continuous coiled crystallizer with hot

and cold zones or other new designs could be an efficient implementation scheme.

Acknowledgments

We are grateful for financial support provided by Merck Research Laboratories and the National Science Foundation (Award No. CTS-0411630). We thank Brian Johnson, Narayan Variankaval and Ivan Santos of Merck Research Laboratories for insightful discussions.

Literature Cited

1. Cussler EL, Moggridge GD, Varma A. *Chemical Product Design*. Cambridge: Cambridge University Press; 2001.
2. Gordon RE, Amin SI. *Crystallization of Ibuprofen*. U.S. Patent Number 4,476,248, 1984.
3. Michaels AS, Colville Jr. AR. The effect of surface active agents on crystal growth rate and crystal habit. *J Phys Chem*. 1960;64:13–19.
4. Weissbuch I, Addadi L, Lahav M, Leiserowitz L. Molecular recognition at crystal interfaces. *Science*. 1991;253:637–645.
5. Zhang Y, Sizemore JP, Doherty MF. Shape evolution of 3-dimensional crystals. *AIChE J*. 2006;52:1906–1915.
6. Snyder RC, Doherty MF. Crystal shape evolution - dissolution and growth. *AIChE J*. 2007;53:1337–1348.
7. Winn D, Doherty MF. A new technique for predicting the shape of solutions-grown organic crystals. *AIChE J*. 1998;44:2501–2514.

Manuscript received July 6, 2006, and revision received Feb. 21, 2007.